Available online at www.sciencedirect.com
ScienceDirect
Nonlinear Analysis: Real World Applications 10 (2009) 1480–1489
Nonlinear Analysis
Real World Applications
www.elsevier.com/locate/nonrwa

Adaptive sliding mode control of a high-precision ball-screw-driven stage

Her-Terng Yau[a,*], Jun-Juh Yan[b]

[a] Department of Electrical Engineering, Far-East University, No 49 Jung-Haw Road, Hsin-Shih Town, Tainan 744, Taiwan, ROC
[b] Department of Computer and Communication, Shu-Te University, Kaohsiung 824, Taiwan, ROC

Received 7 November 2007; accepted 15 January 2008

Abstract

High-precision position control has been widely used in scientific instruments and semiconductor fabrication equipment. Traditionally, controllable displacements with sub-micron and nano-level resolution are usually achieved by piezoelectric actuators because of their high bandwidth and ease of control. However, the travel range of piezoelectric actuator is usually small. In this paper, the ball-screw-driven system is studied to provide long-range and high-precision performance for positioning and tracking control. In such a system, the friction dynamics are divided into the static and the dynamic regimes to describe the dynamic behavior of a conventional ball-screw-driven x-y stage. The same form of adaptive sliding mode controllers are designed in the static and dynamic regimes to obtain the precision performance for controlled stage. A proportional-integral switching surface is proposed to make it easy to assign the performance of the systems in the sliding mode motion and the controller is robust without knowing the bound of disturbance in advance. An illustrative example is included to demonstrate that the system achieves high precision (10 nm) and long-range (10 cm) positioning performance with repeatability and robustness by the proposed control approach.

Keywords: High-precision control; Nano-stage; Adaptive sliding mode control; Friction dynamics

1. Introduction

In recent years, due to the rapid progress in biochemistry, semiconductor and optronics, extremely high-precision positioning control technique has become an important part of the development of precision machines. Many researches have been conducted to characterize and control system behavior under micro/nano-scales in mechanics system. Among others, the ball-screw-driven mechanism actuated by servo drives has widely been used in many applications due to its low cost and generality. However, the main difficulties dealing with positioning problems in a ball-screw-driven mechanism with extremely high precision are the friction behavior. Conventionally, friction behavior can be divided into two regimes: static friction and dynamic friction. Many researches have been done to investigate and model friction dynamics [1–5]. It shows that the dynamic behavior of friction in microscopic displacement is more complex than the traditional macroscopic Coulomb description. Many different phenomena

* Corresponding author. Fax: +886 6 5977570.
E-mail addresses: pan1012@ms52.hinet.net (H.-T. Yau), jjyan@mail.stu.edu.tw (J.-J. Yan).

1468-1218/$ - see front matter © 2008 Elsevier Ltd. All rights reserved.
doi:10.1016/j.nonrwa.2008.01.025

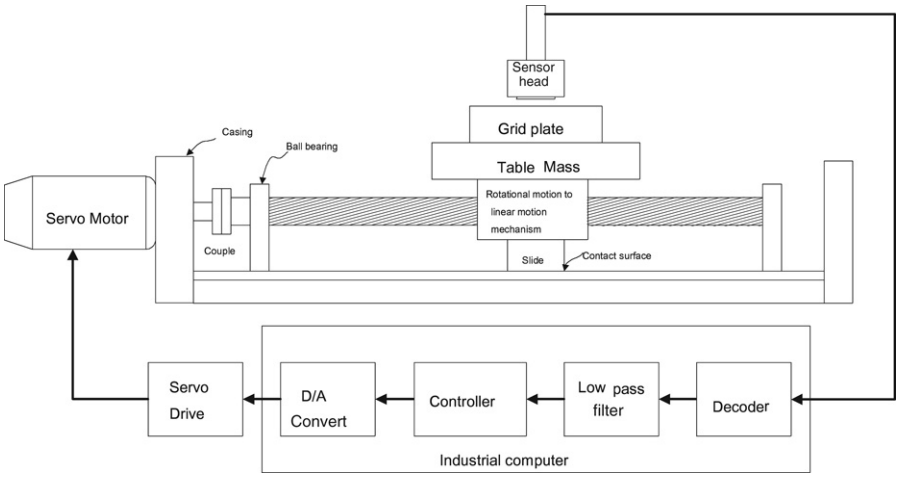

Fig. 1. The schematic diagram of the single-axis ball-screw-driven stage.

such as hysteresis, Stribeck effect, and plasticity have been reported. It deepens the difficulties of high-precision positioning control.

In control applications, compensation for friction is the paradigm to achieve high-precision performance. It is worth to notice that the steady-state positioning error or tracking lag will exist if friction is not well compensated. In the recent researches, Yang and Tomizuka [6] compensated for friction by adaptively changing the control pulse width to cancel out the influence of stiction and coulomb friction. Tung et al. [7] compensated for friction with a repetitive control law. Ro et al. [8] proposed a controller based on the friction observer and a disturbance observer and implemented for sub-micrometer motion. Pan used a PID controller design on a model [9] for angular positioning control. Chen et al. [10] took two friction models to describe the ball-screw-system behavior according to the static and dynamic friction regimes. The sliding mode controller is designed in that paper for positioning control with high precision and long-rang requirements. Besides, the intelligent control schemes such as learning control and fuzzy control have been proposed in [11,12].

In the above control literature, most researches did not divide the friction behavior into static and dynamic regimes to design the controllers. It caused steady-state position error and tracking lag when the friction is not properly compensated and the high-precision control cannot be arrived. In some research, the controllers design is divided into static and dynamic regimes such as Chen et al. [10]. Nevertheless, the control design technique should know the bound of external disturbance in advance. In this paper, positioning control based on the friction model [5] is investigated. The major contribution of this work is that the same types of controllers are applied to the dynamics of the static and the dynamic frictions to reduce the complex and inconvenient controller design scheme. The controller designs are carried out by the adaptive sliding mode control (ASMC) method to obtain attractive advantages, e.g. fast response, good transient performance and insensitive to variation in plant parameters or external disturbances. In order to achieve this goal, proportional-integral switching surfaces for both dynamic and static friction regions are newly proposed to make it easy to assign the performance of the systems in the sliding mode motion. Finally the performances of the system are demonstrated by using a ball-screw-driven servo system to verify our results.

The notations are used throughout this report. $\lambda(W)$ denotes any eigenvalue of the matrix W.$\lambda_{\max}(W)$ represents the maximum value of $\lambda_i(W), i = 1, \ldots, n$. $|W|$ denote the absolute value of scale W.$\mathrm{sgn}(y)$ is the sign function of y, if $s > 0$, $\mathrm{sgn}(y) = 1$; if $s = 0$, $\mathrm{sgn}(y) = 0$; if $s < 0$, $\mathrm{sgn}(y) = -1$.

2. Overall system layout

The schematic diagram of single-axis ball-screw-driven stage considered in this paper is shown in Fig. 1 [10].

To design the control, we first introduce the friction models proposed by Hsieh and Pan [5].

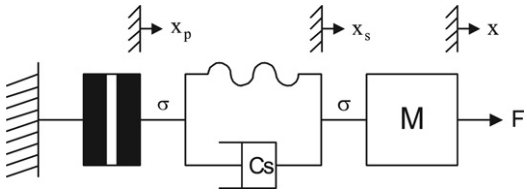

Fig. 2. The simple concept of static friction model.

2.1. Static friction model

Based on the model in [5], the static friction is modeled as the nonlinear spring module and the plastic module. A simple conceptual model of static friction is shown in Fig. 2, where σ is a friction force and it will arise when an external force F is applied. Firstly, the nonlinear spring module is considered and σ_S is the external force and x_S be the displacement of the spring. Therefore, the dynamics equation of the nonlinear spring is

$$\frac{\mathrm{d}\sigma_s}{\mathrm{d}x_s} = k_1 + k_2 \mathrm{e}^{-\beta|x_s - x_r|} \tag{1}$$

where k_1, k_2 and β are positive scalars and x_S denotes the active reverse point state. The above equation resulted in the hysteresis behavior. In the part of plastic module, the governing equation of the plastic deformation is represented as:

$$\begin{cases} \dot{x}_h = \begin{cases} \alpha\left[f(|\sigma|) - x_h\right], & \text{if } f(|\sigma|) > x_h \\ 0, & \text{otherwise} \end{cases} \\ \dot{x}_p = \operatorname{sgn}(\sigma) \cdot \dot{x}_h, \end{cases} \tag{2}$$

where x_h is the hardening state, σ be the applied force, x_p be the plastic deformation, $f(|\sigma|) = \frac{|\sigma^n|}{\lambda}$, and α, λ, n are positive numbers.

The entire system governing equation of static friction is separated into two phases: one is the creep phase; the other is the hardening phase. The state equation is stated as follows

The creep phase: $(\frac{|\sigma|^n}{\lambda} > x_h)$

$$\frac{\mathrm{d}}{\mathrm{d}t}\begin{bmatrix} x_s \\ \dot{x}_s \\ x_h \\ \dot{x}_h \\ x_p \\ \dot{x}_p \end{bmatrix} = \begin{bmatrix} \dot{x}_s \\ \left(1 + \dfrac{\alpha n}{\lambda}|\sigma|^{n-1} C_s\right)^{-1}\left(\dfrac{F-\sigma}{m} - q\right) \\ \dfrac{\alpha|\sigma|^n}{\lambda} - \alpha x_h \\ \operatorname{sign}(\sigma)\left(1 + \dfrac{\alpha n}{\lambda}|\sigma|^{n-1} C_s\right)^{-1}\left(\dfrac{\alpha n}{\lambda}|\sigma|^{n-1} C_s \dfrac{F-\sigma}{m} + q\right) \\ \operatorname{sign}(\sigma)\left(\dfrac{\alpha|\sigma|^n}{\lambda} - \alpha x_h\right) \\ \left(1 + \dfrac{\alpha n}{\lambda}|\sigma|^{n-1} C_s\right)^{-1}\left(\dfrac{\alpha n}{\lambda}|\sigma|^{n-1} C_s \dfrac{F-\sigma}{m} + q\right) \end{bmatrix}. \tag{3}$$

The hardening phase: $(\frac{|\sigma|^n}{\lambda} \le x_h)$

$$\frac{\mathrm{d}}{\mathrm{d}t}\begin{bmatrix} x_s \\ \dot{x}_s \\ x_h \\ \dot{x}_h \\ x_p \\ \dot{x}_p \end{bmatrix} = \begin{bmatrix} \dot{x}_s \\ \dfrac{F-\sigma}{m} \\ 0 \\ 0 \\ 0 \\ 0 \end{bmatrix}. \tag{4}$$

Fig. 3. The schematic concept of bristle model [8].

where

$$\sigma = C_s\dot{x}_s + k_1(x_s - x_r) + \text{sign}(x_s - x_r)\frac{k_2}{\beta}(1 - \text{e}^{-\beta|x_s - x_r|}) + \sigma_r$$

$$q = \frac{\alpha n}{\lambda}|\sigma|^{n-1}(k_1 + k_2\text{e}^{-\beta|x_s - x_r|})\dot{x}_s - \text{sign}(\sigma)\alpha\dot{x}_h.$$

The displacement of system in static friction region is:

$$x = x_s + x_p. \tag{5}$$

Combining the above equations, the response of static friction behavior can be obtained. The parameter values presented in the equations can be identified from the experimental data, and it is quoted from [10] in this paper.

2.2. Dynamic friction model

To describe the dynamic friction behavior, a friction model proposed by Canudas et al. [13] is illustrated in Fig. 3. The friction interface is modeled as elastic bristles. Under such friction load, the system dynamics can be described as

$$m\ddot{x} = F - F_f. \tag{6}$$

where x denotes the displacement of the system. The viscous friction F_f is

$$F_f = \sigma_0 + \sigma_1\dot{z} + \sigma_2 v, \tag{7}$$

where v and z are the relative velocity and bristle deformation, and σ_0 denotes the bristle stiffness, σ_1 and σ_2 denote the damping and the viscous coefficients, respectively. The governing equation of bristle deformation is stated as

$$\dot{z} = v - \frac{|v|}{(F_c + (F_s - F_c)\text{e}^{-(v/v_s)^2})}\sigma_0 z, \tag{8}$$

where F_C denotes the coulomb friction, F_S is the maximum static friction, and v_c denotes the Stribeck velocity defined in [13]. The parameter values of Eqs. (6)–(8) can be determined from the experimental data and it is quoted from [10] in this paper.

3. Adaptive sliding mode controller (ASMC) design

3.1. ASMC for static friction regime

For tracking control purpose, the error state is defined as

$$e = x - x_d, \tag{9}$$

where x_d is the desired system displacement and assume it to be twice differentiable with respect to time. From Eqs. (3)–(5), the following error dynamics equation is obtained:

$$\begin{bmatrix}\dot{e}_1\\ \dot{e}_2\end{bmatrix} = \begin{bmatrix}0 & 1\\ -\dfrac{k_1}{m} & -\dfrac{C_s}{m}\end{bmatrix}\begin{bmatrix}e_1\\ e_2\end{bmatrix} + \begin{bmatrix}0\\ \dfrac{1}{m}\end{bmatrix}F + \begin{bmatrix}d_1(x_s, \dot{x}_s, x_h, \dot{x}_h, x_p, \dot{x}_p, x_r, \sigma_r)\\ d_2(x_s, \dot{x}_s, x_r, \sigma_r)\end{bmatrix}, \tag{10}$$

where $e_1 = x - x_d$ and $e_2 = \dot{e}_1 = \dot{x} - \dot{x}_d$. If the measure tolerance is considered as:

$$\Delta m = m_0 - m_t, \qquad \Delta k_1 = k_{1,0} - k_{1,t}, \qquad \Delta k_2 = k_{2,0} - k_{2,t}, \qquad \Delta C_s = C_{s,0} - C_{s,t},$$
$$\Delta\beta \equiv \beta_0 - \beta_t, \qquad \Delta\alpha \equiv \alpha_0 - \alpha_t, \qquad \Delta n \equiv n_0 - n_t, \qquad \Delta\lambda \equiv \lambda_0 - \lambda_t,$$

where the subscript '0' denotes the value of nominal system and 't' denotes the parameter value of real system. Then the system (10) can be rewritten as

$$\begin{bmatrix}\dot{e}_1\\ \dot{e}_2\end{bmatrix} = \begin{bmatrix}0 & 1\\ -\dfrac{k_1}{m} & -\dfrac{C_s}{m}\end{bmatrix}\begin{bmatrix}e_1\\ e_2\end{bmatrix} + \begin{bmatrix}0\\ \dfrac{1}{m}\end{bmatrix}F + \begin{bmatrix}d_1 + \Delta d_1\\ d_2 + \Delta d_2 + \sum(x_d, \dot{x}_d, \ddot{x}_d)\end{bmatrix}, \tag{11}$$

where $\Delta d_1 = \Delta d_1(\Delta m, \Delta k_1, \Delta k_2, \Delta C_s, \Delta\beta, \Delta\alpha\Delta n, \Delta\lambda)$and $\Delta d_2 = \Delta d_2(\Delta m, \Delta k_1, \Delta k_2, \Delta C_s, \Delta\beta)$, and it can be in a general form as

$$\dot{E} = \begin{bmatrix}\dot{e}_1\\ \dot{e}_2\end{bmatrix} = AE + BF + D, \tag{12}$$

where

$$A = \begin{bmatrix}0 & 1\\ \dfrac{-k_1}{m} & \dfrac{-C_s}{m}\end{bmatrix}, \qquad B = \begin{bmatrix}0\\ \dfrac{1}{m}\end{bmatrix}, \qquad D = \begin{bmatrix}\hat{d}_1\\ \hat{d}_2\end{bmatrix},$$
$$\hat{d}_1 = d_1 + \Delta d_1, \quad \text{and} \quad \hat{d}_2 = d_2 + \Delta d_2 + \sum(x_d, \dot{x}_d, \ddot{x}_d). \tag{13}$$

Firstly, the switching surface is defined as

$$s = CE - \int_0^t (CA + CBK)E(\tau)\mathrm{d}\tau, \tag{14}$$

where $C, K \in R^{1\times 2}$ are selected to satisfy $CB \neq 0, \lambda_{\max}(A + BK) < 0$. It is known [15–17] that as long as the system operates in the sliding mode, it satisfies the equations

$$\dot{s}(t) = 0 \quad \text{and} \quad s(t) = 0. \tag{15}$$

Therefore, the equivalent control F_{eq} in the sliding manifold can be obtained. By differentiating (14) with respect to time and substituting from (11), then

$$\dot{s} = 0 = CBF_{eq} + CD - CBKE = 0 \tag{16}$$
$$\Rightarrow F_{eq} = KE - (CB)^{-1}CD. \tag{17}$$

Substituting F_{eq} into (12), the following sliding mode equation is obtained as

$$\begin{aligned}\dot{E} &= (A + BK)E + (I - B(CB)^{-1}C)D\\ &= (A + BK)E + PD.\end{aligned} \tag{18}$$

According to [5], the creep motion will finally vanish if the applied force is not monotonic increasing or decreasing. Such a property could conclude that the controlled system will enter the hardened phase, i.e. the uncertain will turn into matching condition and can be totally rejected by the adaptive sliding mode control.

Once a proper switching surface has been selected with the appropriate matrices C and K, it should do next is to design an adaptive variable structure controller, which is not only derive the system trajectories onto the sliding surface but also remove the limitation value of the knowing uncertainties in advance.

Before proceeding to the adaptive sliding mode control design, the Barbalat lemma is provided:

Lemma 1 *((Barbalat Lemma)[18]). If $\tilde{w} : R \to R$ is a uniformly continuous function for $t \geq 0$ and if the limit of the integral*

$$\lim_{t\to\infty}\int_0^t |\tilde{w}(\lambda)|\,\mathrm{d}\lambda$$

exists and is finite, then

$$\lim_{t\to\infty} \tilde{w}(t) = 0. \tag{19}$$

To ensure the occurrence of the sliding motion in static friction region, an adaptive variable structure control is proposed as

$$F = -(CB)^{-1}[|CBKE| + \eta\hat{\beta}(t)]\text{sign}(s); \quad \eta > 1. \tag{20}$$

The adaptive law is

$$\dot{\hat{\beta}}(t) = \xi^{-1}|s|; \qquad \hat{\beta}(0) = \hat{\beta}_0; \quad \xi > 0 \tag{21}$$

ywhere $\hat{\beta}_0$ is the bounded positive initial value of $\hat{\beta}(t)$. The adaptive law can be also rewritten in the integral form as

$$\hat{\beta}(t) = \hat{\beta}_0 + \int_0^t \xi^{-1}|s(\tau)|\,\mathrm{d}\tau. \tag{22}$$

In the following, the proposed adaptive scheme (20) and (21) [14] will be proved to be able to derive the uncertain system (12) in the static friction region onto the sliding surface $s(t) = 0$.

Theorem 1. *Consider the dynamics of system (12) in the static friction region, this system is controlled by $F(t)$ in (20) with adaptation law (21). Then the system trajectory converges to the sliding surface $s(t) = 0$.*

Proof. Select Lyapunov function candidate as

$$V(t) = \frac{1}{2}(s^2 + \xi w^2), \tag{23}$$

where $w(t) \in R$ denotes the adaptation error which will be well defined later.

Taking the derivative of $V(t)$ with respect to time t, it has

$$\dot{V}(t) = s\dot{s} + \xi w\dot{w}. \tag{24}$$

By using Eqs. (12) and (14), we obtain

$$\begin{aligned}\dot{V}(t) &= s(CBF + CD - CBKE) + \xi w\dot{w}\\ &\le |s|\,(|CBKE| + |CD|) + sCBF + \xi w\dot{w}.\end{aligned} \tag{25}$$

Assume there exists an upper bound β such that

$$|CD| \le \beta. \tag{26}$$

Define the adaptation error as

$$w(t) = \hat{\beta}(t) - \beta. \tag{27}$$

Inserting (20), (26) and (27) into the right hand of inequality (25), this yields

$$\dot{V}(t) \le \underbrace{(\beta - \hat{\beta}(t))}_{-w}|s| + (1-\eta)\hat{\beta}(t)|s| + \xi w\dot{\hat{\beta}}(t) = -(\eta-1)\hat{\beta}|s|. \tag{28}$$

Now if we define $\tilde{w}(t) = (\eta-1)\hat{\beta}|s|$, and integrating the above equation from zero to t, it yields

$$\begin{aligned}&V(t) \le V(0) - \int_0^t \tilde{w}(\lambda)\mathrm{d}\lambda\\ &\Rightarrow V(0) \ge V(t) + \int_0^t \tilde{w}(\lambda)\mathrm{d}\lambda \ge \int_0^t \tilde{w}(\lambda)\mathrm{d}\lambda.\end{aligned} \tag{29}$$

Table 1
Parameters of the dynamic friction [10]

$k_1 = 6.12 \times 10^6$ (N/m)	$\alpha = 1.64 \times 10^{-2}$
$k_2 = 2.88 \times 10^8$ (N/m)	$C_s = 9.1 \times 10^4$
$\beta = 1.11 \times 10^8$	$\lambda = 9.15 \times 10^6$
$n = 2.283$	

Taking the limit as $t \to \infty$ on both sides of (29) gives

$$\infty > V(0) \geq \lim_{t\to\infty} \int_0^t \tilde{w}(\lambda)\mathrm{d}\lambda. \tag{30}$$

Thus according to Barbalat lemma (see Lemma 1), we obtain

$$\lim_{t\to\infty} \tilde{w}(t) = \lim_{t\to\infty} (\eta - 1)\hat{\beta}\,|s| \to 0. \tag{31}$$

Since $\eta > 1$, $\hat{\beta} > 0$, (29) implies $s(t) \to 0$ as $t \to \infty$. Hence the proof is achieved completely. □

3.2. ASMC for dynamic friction regime

From Eq. (6), the error dynamic in the dynamic friction region can be described as

$$\begin{bmatrix} \dot{e}_1 \\ \dot{e}_2 \end{bmatrix} = \underbrace{\begin{bmatrix} 0 & 1 \\ 0 & 0 \end{bmatrix}}_{A} \begin{bmatrix} e_1 \\ e_2 \end{bmatrix} + \underbrace{\begin{bmatrix} 0 \\ \frac{1}{m} \end{bmatrix}}_{B} F - \underbrace{\begin{bmatrix} 0 \\ \frac{F_f}{m} - \ddot{x}_d \end{bmatrix}}_{D}. \tag{32}$$

According to the design procedure in static friction regime, we define the switching function with the same form as follows

$$s = CE - \int_0^t (CA + CBK)E(\tau)\mathrm{d}\tau, \tag{33}$$

where $C, K \in R^{1\times 2}$ are selected to satisfy

$$CB \neq 0, \lambda_{\max}(A + BK) < 0. \tag{34}$$

In order to ensure the occurrence of the sliding motion in dynamic friction region, an adaptive variable structure control is proposed as

$$F = -(CB)^{-1}[|CBKE| + \eta\hat{\beta}(t)]\mathrm{sign}(s); \quad \eta > 1. \tag{35}$$

The adaptive law is

$$\dot{\hat{\beta}}(t) = \xi^{-1}\,|s|\,; \qquad \hat{\beta}(0) = \hat{\beta}_0; \quad \xi > 0. \tag{36}$$

Owing to the proofs for the stability and hitting of the dynamic friction regime in the sliding mode are similar to that in the static regime, they are omitted here.

Remark 1. The controller in (20) and (35) demonstrate a discontinuous control laws and the phenomenon of chattering will appear. In order to eliminate the chattering, the function of *sign*(s) in (20) and (35) are modified as

$$\mathrm{sign}(s) = \frac{s}{|s| + \delta}, \tag{37}$$

where δ is a sufficiently small design constant. Therefore, the controllers can be implemented in a real word system.

Table 2
Parameter values of the static friction [10]

$\sigma_0 = 1 \times 10^5$ (N/m)	$F_s = 10.8175$ (N)
$\sigma_1 = 316$ (N s/m)	$F_c = 7.5$ (N)
$\sigma_2 = 350$ (N s/m)	$v_s = 0.001$ (m/s)

Table 3
Parameter values of the controllers

Static friction controller	Dynamic friction controller
$C = \begin{bmatrix} 1 & 40.4 \end{bmatrix}$	$C = \begin{bmatrix} 1 & 40.4 \end{bmatrix}$
$K = \begin{bmatrix} 6.1 \times 10^6 & 9.079 \times 10^4 \end{bmatrix}$	$K = \begin{bmatrix} 24240 & 2020 \end{bmatrix}$
$\xi = 0.5$	$\xi = 0.5$
$\eta = 2$	$\eta = 2$
$\hat{\beta}_0 = 10$	$\hat{\beta}_0 = 10$

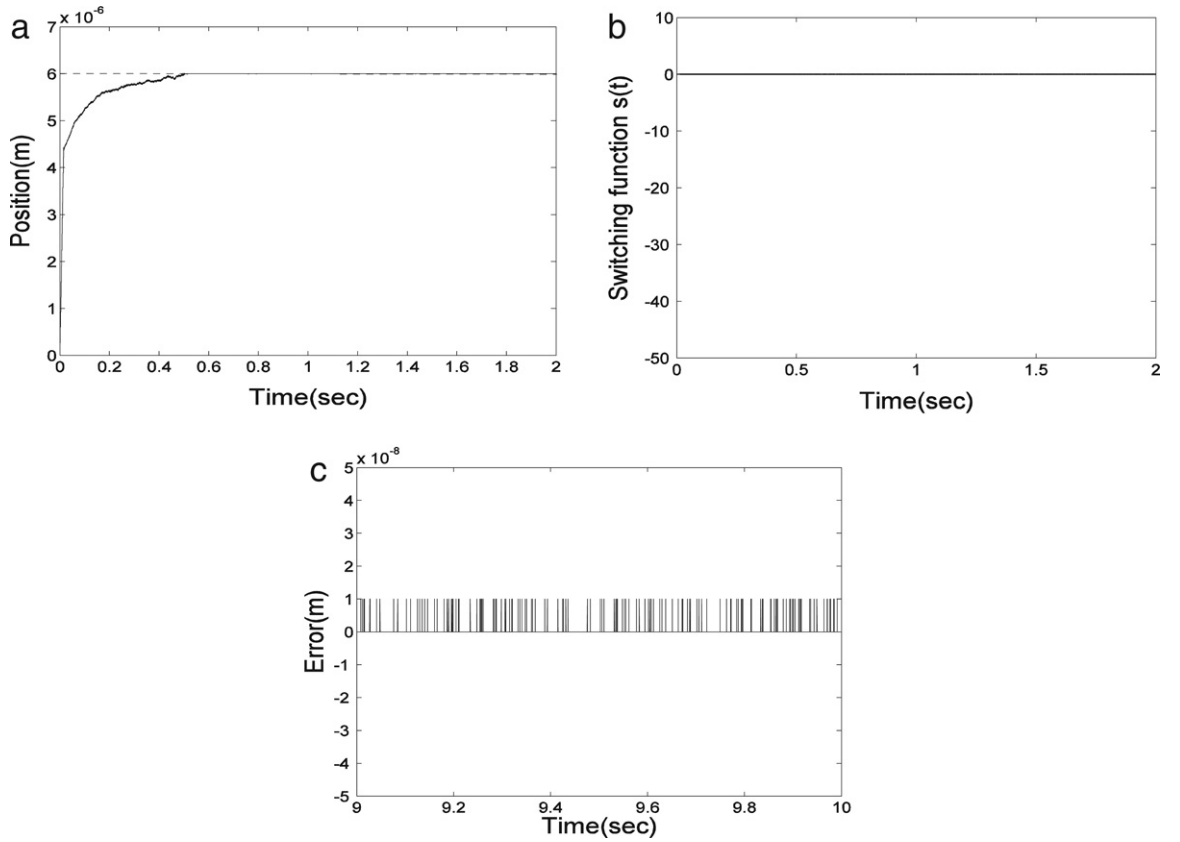

Fig. 4. The positioning response to 6 μm command. (a) The transient time response. (b) The response of switching function. (c) The steady-state error response.

4. Simulation results

In this section, the computer simulation results of a ball-screw-driven stage are given to demonstrate the feasibility of the adaptive sliding mode controller design. Consider the ball-screw-driven stage described in Section 3 with $m = 40.4$ kg, where all the parameters are shown in Tables 1 and 2. In digital control law implementation, there exist system constraints such as sensor resolution and D/A resolution limit, which will restrict system performance.

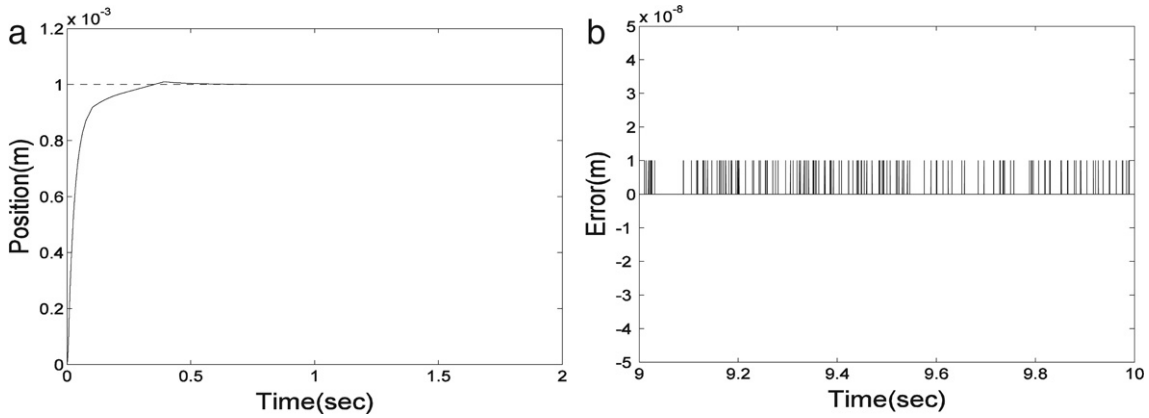

Fig. 5. The positioning response to 1 mm command. (a) The transient time response. (b) The steady-state error response.

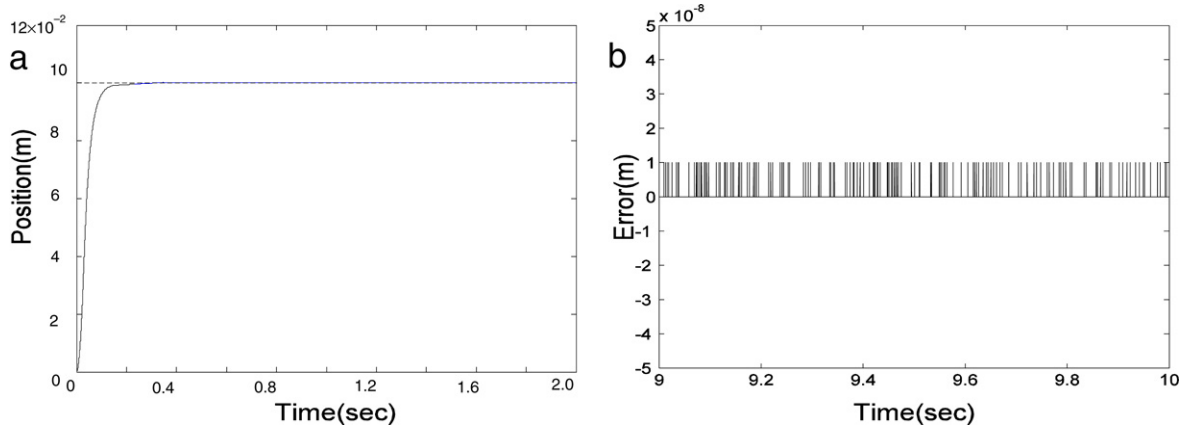

Fig. 6. The positioning response to 10 cm command. (a) The transient time response. (b) The steady-state error response.

In our simulation the value 1 μm is used to switch the control type to static friction controller or dynamic friction controller. To simulate real system response, we utilized a quantization function to specify such limits and the control force is saturated when $|u| \geq 200Nt$. The simulation results with reference command 6 μm, 1 mm and 10 cm with controller parameters in Table 3 are shown in Figs. 4–6. It can be seen that the ball-screw stage is regulated to the reference command successfully about in 1 s, without respect to short range (6 μm), or long range (10 cm). From Figs. 4(c), 5(b), and 6(b), they also show that the steady-state error is less than 10 nm. Therefore, it concludes that the high-precision position control of ball-screw stage can be reached by this controller in this paper.

5. Conclusions

In this paper, two friction models were used to describe the ball-screw-stage-system behavior according to the static and dynamic friction regimes. The adaptive sliding mode control scheme is used to control the system to reach the high-precision position control. Based on the variable structure control theory and Barbalat Lemma, it can be seen that this controller is robust to external disturbance without knowing the bound of disturbance in advance and the proposed controller also guarantees the occurrence of sliding motion for systems in both dynamic and static friction regions. Simulation results show that the ball-screw x-y stage positioning control with high precision and long-range requirements were achieved.

References

[1] A. Banerjee, Influence of kinetic friction on the critical velocity of stick-slip motion, Wear 12 (1968) 107–116.
[2] D. Karnopp, Computer simulation of stick-slip friction in mechanical dynamic systems, J. Dynam. Syst. Meas. Contr. 107 (1985) 100–103.

[3] D. Haessig, B. Friedland, On the modeling and simulation of friction, J. Dynam. Syst. Meas. Contr. 113 (1991) 354–362.
[4] B. Armstrong-Helouvry, P. Dupont, C. Canudas de Wit, A survey of models, analysis tools, and compensation methods for the control of machines with friction, Automatica 30 (7) (1994) 1083–1138.
[5] C. Hsieh, Y.C. Pan, Dynamic behavior and modeling of the pre-sliding static friction, Wear 242 (2000) 1–17.
[6] S. Yang, M. Tomizuka, Adaptive pulse width control for precise positioning under the influence of stiction and coulomb friction, J. Dynam. Syst. Meas. Contr. 110 (1988) 221–227.
[7] E.D. Tung, G. Anwar, M. Tomizuka, Low-velocity friction compensation and feed-forward solution based on repetitive control, J. Dyn. Syst. Meas. Control 115 (1993) 279–284.
[8] P.I. Ro, W. Shim, S. Jeong, Robust friction compensation for submicrometer positioning and tracking for a ball-screw-driven slide system, Prec. Eng. 24 (2000) 160–173.
[9] Y.C. Pan, Investigation of static friction and high precision positioning control, Ph.D. Thesis, Department of Aeronautical and Astronautical Engineering, Cheng Kung University, Tainan Taiwan, June, 2000.
[10] C.L. Chen, M.J. Jang, K.C. Lin, Modeling and high-precision control of a ball-screw-driven stage, Prec. Eng. 28 (2004) 483–495.
[11] S. Cetinkunt, A. Donmez, CMAC learning controller for servo control of high-precision machine tools, in: Proceedings of the American Control Conference, June 1993, pp. 1976–1980.
[12] J.T. Teeter, M.W. Chow, J.J. Brickley, A novel fuzzy friction compensation approach to improve the performance of a DC motor control system, IEEE Trans. Indust. Electr. 43 (1) (1996) 113–120.
[13] C. Canudas de Wit, H. Olsson, K.J. Astrom, P. Lischinsky, New model for control of systems with friction, Automat. Control 40 (3) (1995) 419–425.
[14] J. Lu, J. Cao, Adaptive synchronization in tree-like dynamical networks, Nonlinear Anal. R. Word Appl. 8 (2007) 1252–1260.
[15] M.E.M. Meza, A. Bhaya, E. Kaszkurewicz, Stabilizing control of ratio-dependent predator-prey models, Nonlinear Anal. R. Word Appl. 7 (2006) 619–633.
[16] V.I. Utkin, Sliding Mode and their Applications in Variable Structure Systems, Mir Editors, Moscow, 1978.
[17] U. Itkis, Control System of Variable Structure, Wiley, New York, 1976.
[18] V.M. Popov, Hyperstability of Control System, Springer-Verlag, Berlin, 1973.